

Table of Contents

1. Instruments and Materials

2. Experimental Section

3. NMR Spectra

4. HRMS Spetra

5. HPLC Analysis

6. Single Crystal Data

7. Reference

1. Instrumentation and Material

General. All of the chemicals, reagents, and solvents from commercial sources were used as received without further purification unless otherwise noted. Anhydrous tetrahydrofuran (THF), dichloromethane (DCM), and diethyl ether (Et₂O) were obtained by distillation over sodium or CaH₂. Column chromatography was carried out on silica gel (200–300 mesh).

¹H and ¹³C nuclear magnetic resonance (NMR) spectra were recorded on a Bruker AVIII-500 spectrometer (500 MHz and 125 MHz, respectively) or Bruker AVIII-850 spectrometer at 298 K (850 MHz and 213 MHz, respectively). The spectra were referenced to residual proton-solvent references (¹H: CDCl₃: 7.26 ppm, benzene-d₆: 7.16 ppm; ¹³C: CDCl₃: 77.23 ppm, benzene-d₆: 128.62 ppm). High-resolution mass spectra (HRMS) were recorded on a Bruker En Apex Ultra 7.0T FTMS mass spectrometer. High-performance liquid chromatography (HPLC) analyses were performed on a Shimadzu LC-16A instrument, using Daicel Chiralcel IE Columns. Circular dichroism (CD) spectra were recorded on JASCO J-810 circular dichroism spectrometer at 298 K. All CD spectra of the separated enantiomers were measured in ethyl acetate. Single crystal X-ray diffraction data were collected on Rigaku SuperNova X-Ray single crystal diffractometer using Cu K α ($\lambda = 1.54184 \text{ \AA}$) micro-focus X-ray sources at 150 K.

A list of abbreviations:

rt: room temperature

DCM: dichloromethane

DMF: N,N-dimethylformamide

DMSO: dimethyl sulfoxide

EA: ester acetate

PE: petrol ether

THF: tetrahydrofuran

CD: circular dichroism

HPLC: high-performance liquid chromatography

NMR: nuclear magnetic resonance

DEPT: distortionless enhancement by polarization transfer

COSY: correlation spectroscopy

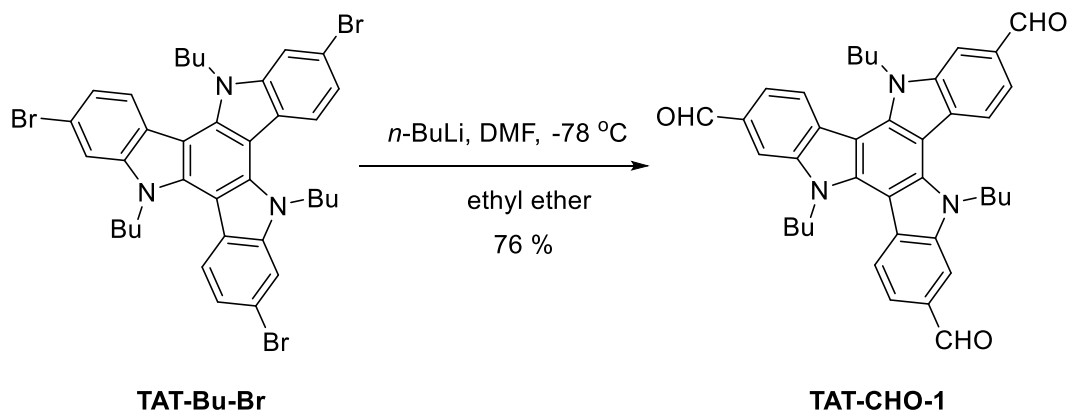
HSQC: heteronuclear single-quantum correlation

HMBC: ¹H detected heteronuclear multiple bond correlation

NOESY: nuclear Overhauser enhancement spectroscopy

2. Experimental Section

2,7,12- trialdehyde-5,10,15-tributyl- triazatruxene (TAT-CHO-1)

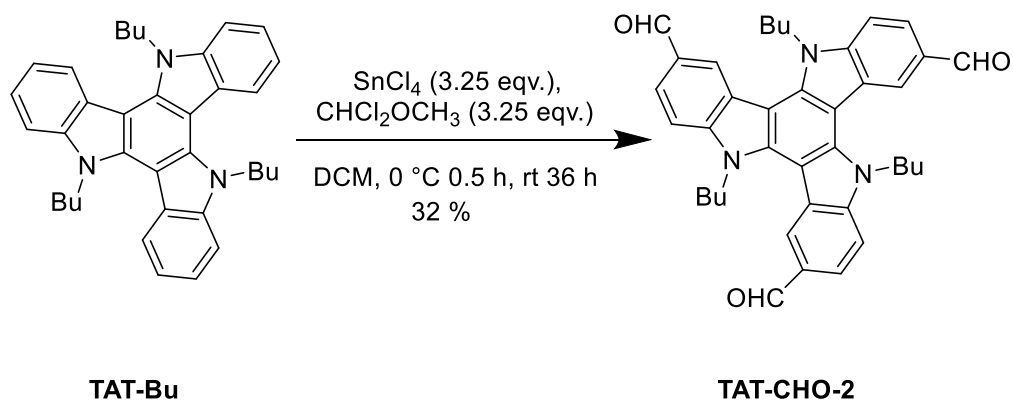


Scheme S1. Synthetic route of **TAT-CHO-1**.

Procedure: **TAT-Bu-Br** (102 mg, 0.14 mmol) was dissolved in anhydrous ethyl ether (10.0 mL) and cooled to $-78\text{ }^{\circ}\text{C}$ under N_2 atmosphere. Then $n\text{-BuLi}$ (0.85 mL, 2.1 mmol, 2.4 M in hexane) was added dropwise and stirred for 30 min at $-78\text{ }^{\circ}\text{C}$. The mixture was stirred for 30 min at $0\text{ }^{\circ}\text{C}$, then warmed to room temperature for another 30 min. After that, the mixture was cooled to $-78\text{ }^{\circ}\text{C}$ again, followed by slow addition of anhydrous DMF and overnight stirring at that temperature. Then the reaction mixture was warmed to room temperature and hydrochloric acid (2 mol/L, 15 mL) was added. A yellow crude product was obtained after extraction by DCM. The crude product was purified by recrystallization using CHCl_3/PE (v/v = 1/8) as mixed solution to give a yellow pure product **TAT-CHO-1** (61 mg, 76 %).¹⁻²

$^1\text{H NMR}$ (500 MHz, CDCl_3) δ 10.22 (s, 3H), 8.38 (d, $J = 8.3$ Hz, 3H), 8.20 (s, 3H), 7.91 (d, $J = 8.3$ Hz, 3H), 5.04 – 4.99 (t, 6H), 1.98 (m, 6H), 1.28 (m, 6H), 0.88 (t, 9H). $^{13}\text{C NMR}$ (125 MHz, CDCl_3) δ 192.17, 142.23, 140.63, 131.74, 128.23, 122.99, 121.60, 111.17, 103.46, 47.42, 32.19, 20.11, 13.90. HRMS (m/z): $[\text{M}+\text{Na}]^+$ calcd for $\text{C}_{39}\text{H}_{39}\text{N}_3\text{O}_3\text{Na}$, 620.28836; found, 620.28872.

3,8,13-trialdehyde-5,10,15-tributyl- triazatruxene (**TAT-CHO-2**)



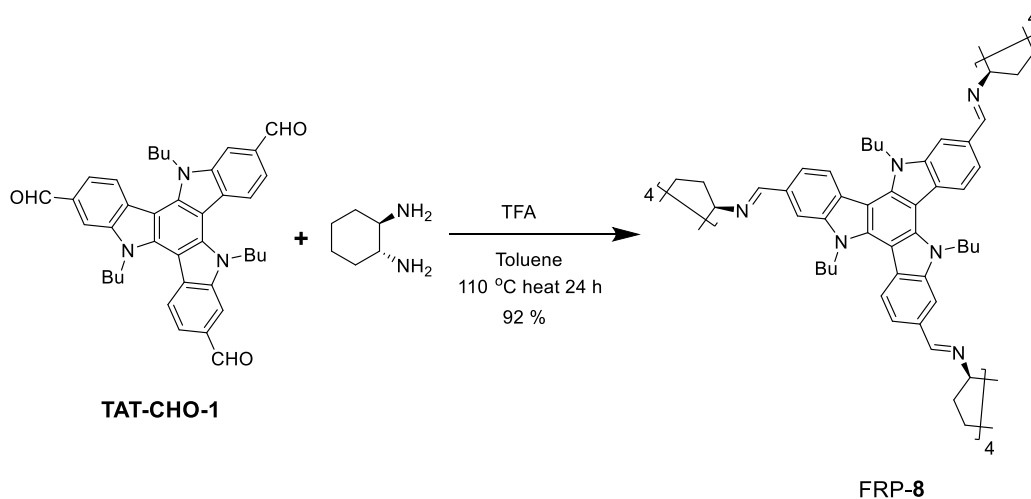
Scheme S2. Synthetic route of **TAT-CHO-2**.

Procedure: **TAT-Bu**³ (0.411 g, 0.80 mmol) was dissolved in anhydrous DCM (10.0 mL) and cooled to $0\text{ }^{\circ}\text{C}$ under N_2 atmosphere. Tin(IV) chloride (SnCl_4) (0.31

mL, 2.60 mmol, 3.25 eqv.) was added dropwise to the solution while stirring, followed by slow addition of dichloromethyl methyl ether (0.23 mL, 2.60 mmol, 3.25 eqv.). The solution was stirred at 0 °C for 30 min, then warmed to room temperature and stirred for another 36 h. The dark solution was diluted with DCM (10 mL) and poured into a funnel filled with ice and shaken thoroughly. The organic layers were separated, and the aqueous phase was diluted with water (10 mL) and extracted with DCM (3 × 10 mL). The combined organic layers were washed with water (2 × 100 mL) and saturated aqueous sodium bicarbonate (2 × 100 mL), and saturated aqueous sodium chloride (200 mL). The organic layer was dried with anhydrous sodium sulfate, and the solvents were removed under reduced pressure to give the crude product as a dark red oil. The crude product was purified on a silica gel column using EA/DCM/PE (v/v/v = 1/1/2) as eluent to give a yellow product (0.153 g, 32%).⁴

¹H NMR (500 MHz, CDCl₃) δ 10.17 (s, 3H), 8.78 (s, 3H), 8.01 (dd, *J*₁ = 8.4 Hz, *J*₂ = 1.0 Hz, 3H), 7.72 (d, *J* = 8.4 Hz, 3H), 4.97 – 4.92 (t, 6H), 2.04 (m, 6H), 1.39 (m, 6H), 0.92 (t, 9H). ¹³C NMR (125 MHz, CDCl₃) δ 191.82, 144.78, 139.73, 129.76, 126.22, 124.20, 123.01, 110.94, 104.03, 77.41, 77.16, 76.91, 47.40, 32.40, 20.05, 13.94. HRMS (*m/z*): [M+Na]⁺ calcd for C₃₉H₃₉N₃O₃Na, 620.28836; found, 620.29041.

Imidization reaction of TAT-CHO-1 and (1R,2R)-CHDA to [4+6] cage (FRP-8)⁵:



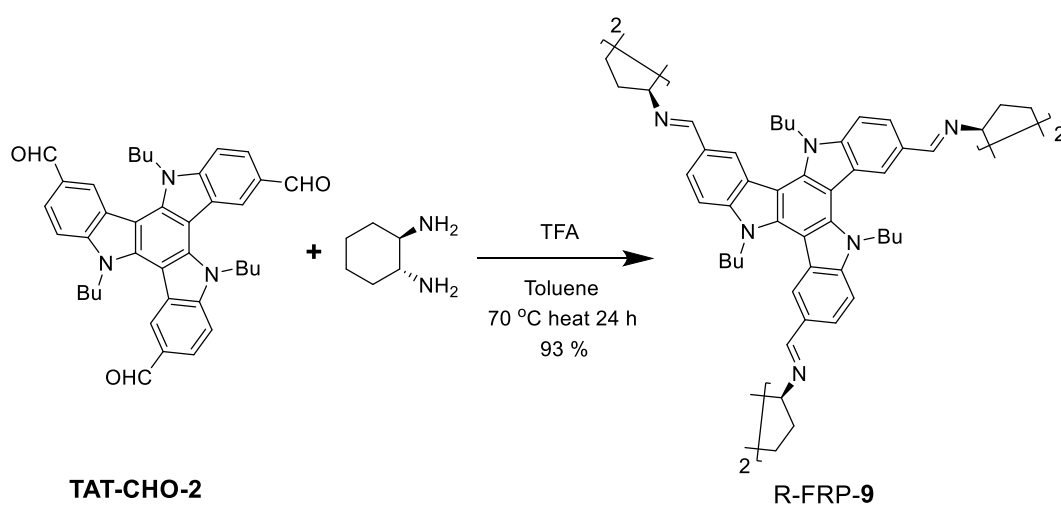
Scheme S3. Synthetic route of FRP-8.

Procedure: TAT-CHO-1 (20 mg, 0.033 mmol) dissolved in toluene (30 mL, 0.67 mg/mL) was drop added into (1R,2R)-CHDA (0.051 mmol, 1.5 × 1.05 eqv.) dissolved in toluene (30 mL), then trifluoroacetic acid (TFA) (0.29 mg, 0.075 eqv.) was added to the solution. The mixture was stirred for about 24 h at 110 °C. The yellow solution was filtered and the solvents were removed under reduced pressure to gave the crude product as a yellow solid. The crude product was purified by IE Columns using toluene/EA = 1/4 (v/v = 1/4) as eluent to gave five stereoisomers FRP-8 (17.3 mg,

92 %). Ratio of (CCCC)-FRP-8, (CCCA)-FRP-8, (CCAA)-FRP-8, (CAAA)-FRP-8, and (AAAA)-FRP-8 was determined by chiral HPLC to be 8:23:27:15:18. We have carried out this condensation reaction at different concentrations (**TAT-CHO-1**). At higher concentrations (1 mg/mL), the reaction gave [4+6] polyhedra as main assembly product, but due to the low solubility of **TAT-CHO-1**, the reaction also produced yellow precipitates which are unsoluble oligomers. At lower concentrations (0.4 mg/mL and 0.25 mg/mL), the reaction gave only [4+6] polyhedra and no other assembly was found by MS. The concentrations reported here (0.67 mg/mL) are the highest concentration that give no apparent side reaction.

HRMS (m/z): $[M+2H]^{2+}$ calcd for $C_{192}H_{218}N_{24}$, 1430.89240; Found, 1430.89803.

Imidization reaction of **TAT-CHO-2** and (1R,2R)-CHDA to [2+3] prime (**FRP-9**)⁵:



Scheme S4. Synthetic route of R-FRP-9.

Procedure: Compound **TAT-CHO-2** (20 mg, 0.033 mmol) dissolved in toluene (20 mL, 1 mg/mL) was drop added to (1R,2R)-CHDA (0.051 mmol, 1.5×1.05 eqv.) dissolved in toluene (20 mL), then trifluoroacetic acid (TFA) (0.29 mg, 0.15 eqv.) was added to the solution. The mixture was stirred for 24 h at 70 °C. The yellow solution was filtered and the solvents were removed under reduced pressure to give the crude product as a yellow solid. The crude product was purified by IE Columns using EtOH/hexane = 1/4 (v/v = 1/4) as eluent to give a pale yellow product **R-FRP-9** (17.8 mg, 93 %). We have carried out this condensation reaction at different concentrations (**TAT-CHO-2**). At higher concentrations (1.75 mg/mL), the reaction gave [2+3] prism as main assembly product, but due to the low solubility of **TAT-CHO-2**, the reaction also produced yellow precipitates which are unsoluble oligomers. At lower concentrations (0.4 mg/mL and 0.25 mg/mL), the reaction gave only [2+3] polyhedra and no other assembly was found by MS. The concentrations reported here (1 mg/mL) are the highest concentration that give no apparent side reaction. The assembly of **TAT-CHO-2** and (1S,2S)-CHDA was carried out using the same synthetic procedure to give S-FRP-9.

¹H NMR (600 MHz, $CDCl_3$) δ 8.18 (d, $J = 8.3$ Hz, 3H), 7.81 (s, 3H), 7.50 (d, $J = 8.4$

Hz, 3H), 7.13 (s, 3H), 4.05 – 4.07 (m, 3H), 3.74 – 3.77 (m, 3H), 3.26 (d, $J = 9.8$ Hz, 3H), 2.30-2.33 (m, 3H), 2.10 – 2.12 (m, 3H), 2.00 (t, 3H), 1.75 – 1.70 (m, 3H), 1.62 (t, 3H), 1.57 – 1.52 (m, 3H), 1.16 (m, 6H), 0.88 (t, $J = 7.4$ Hz, 9H). ^{13}C NMR (150 MHz, CDCl_3) δ 165.58, 141.79, 137.44, 128.20, 125.71, 121.41, 120.73, 110.28, 102.41, 73.33, 46.51, 32.85, 32.48, 24.88, 20.05, 14.04. HRMS (m/z): $[\text{M}+\text{H}]^+$ calcd for $\text{C}_{96}\text{H}_{109}\text{N}_{12}$, 1430.89240; Found, 1430.90521.

3. NMR Spectra

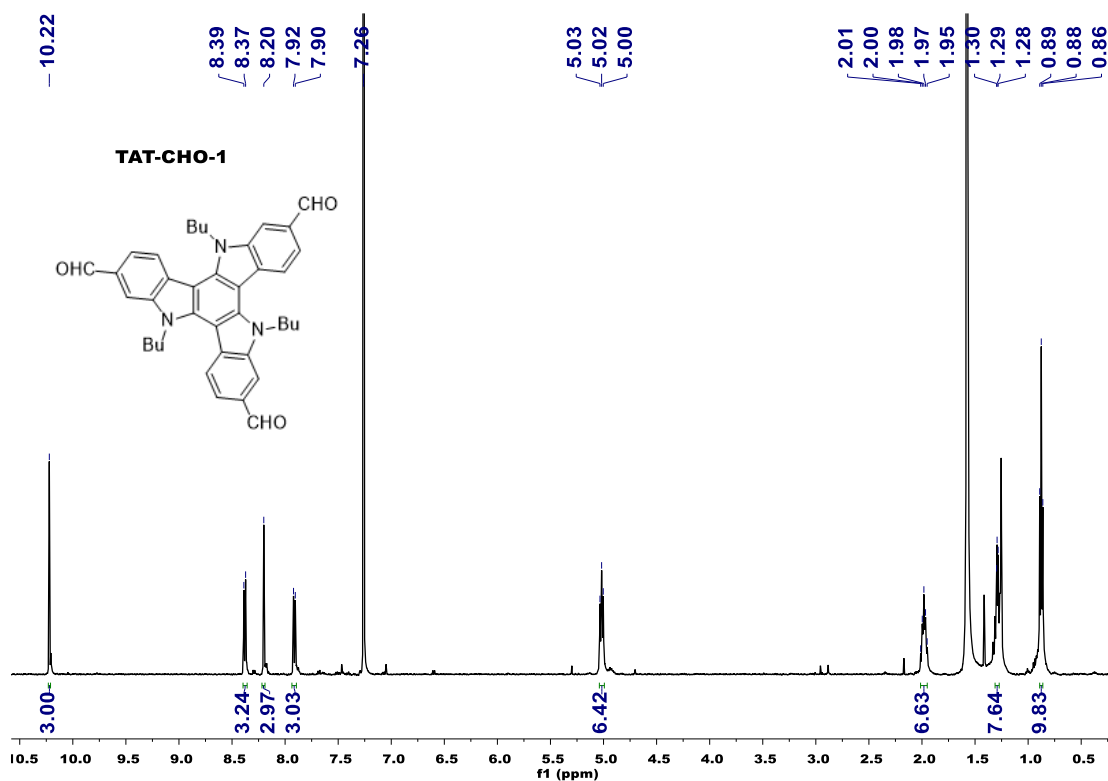


Figure S1. ^1H NMR spectrum of TAT-CHO-1.

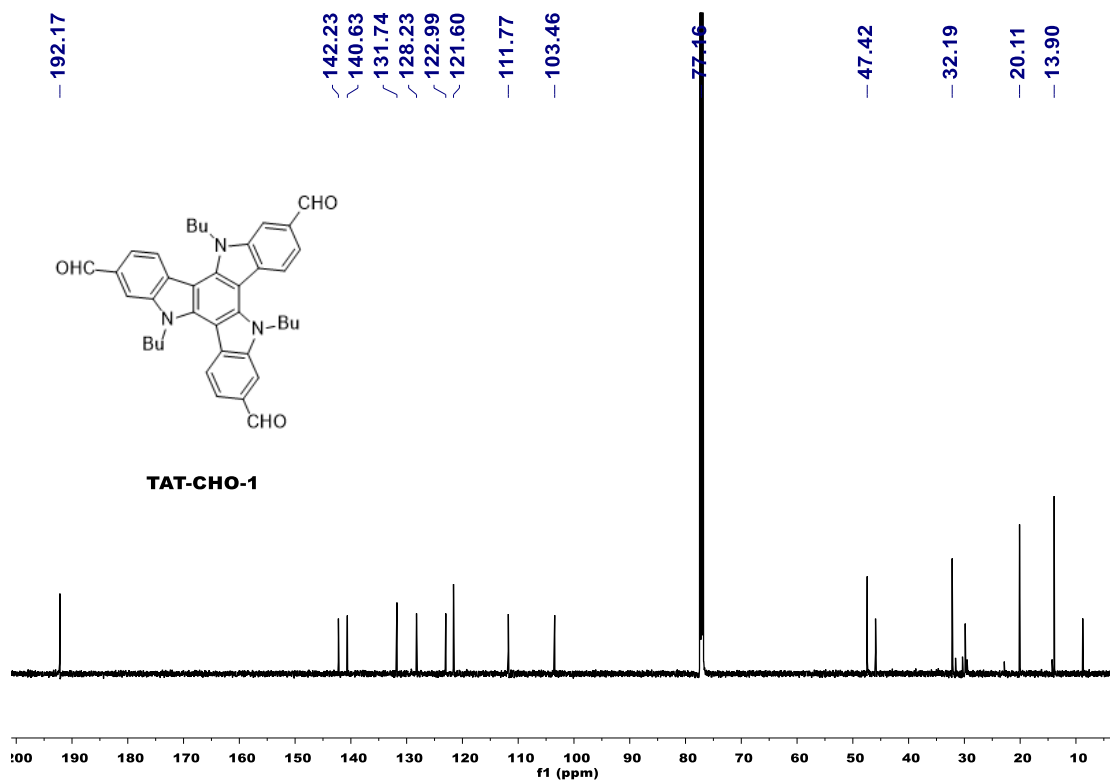


Figure S2. ^{13}C NMR spectrum of TAT-CHO-1.

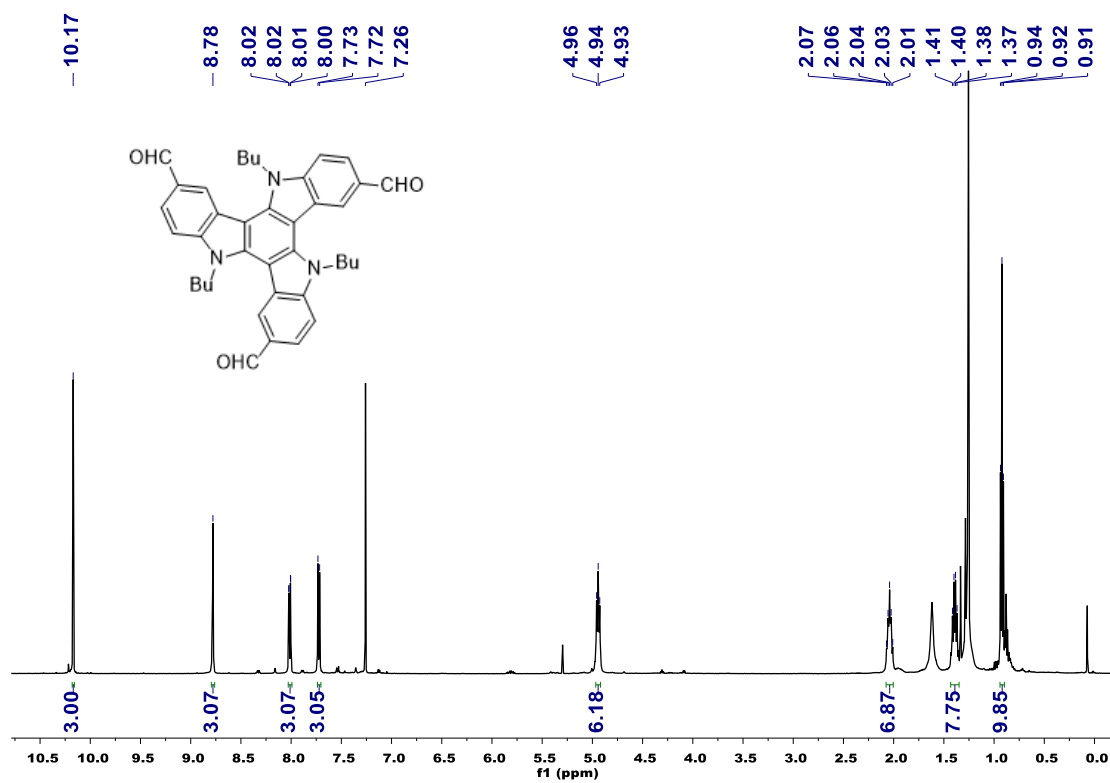


Figure S3. ^1H NMR spectrum of TAT-CHO-2.

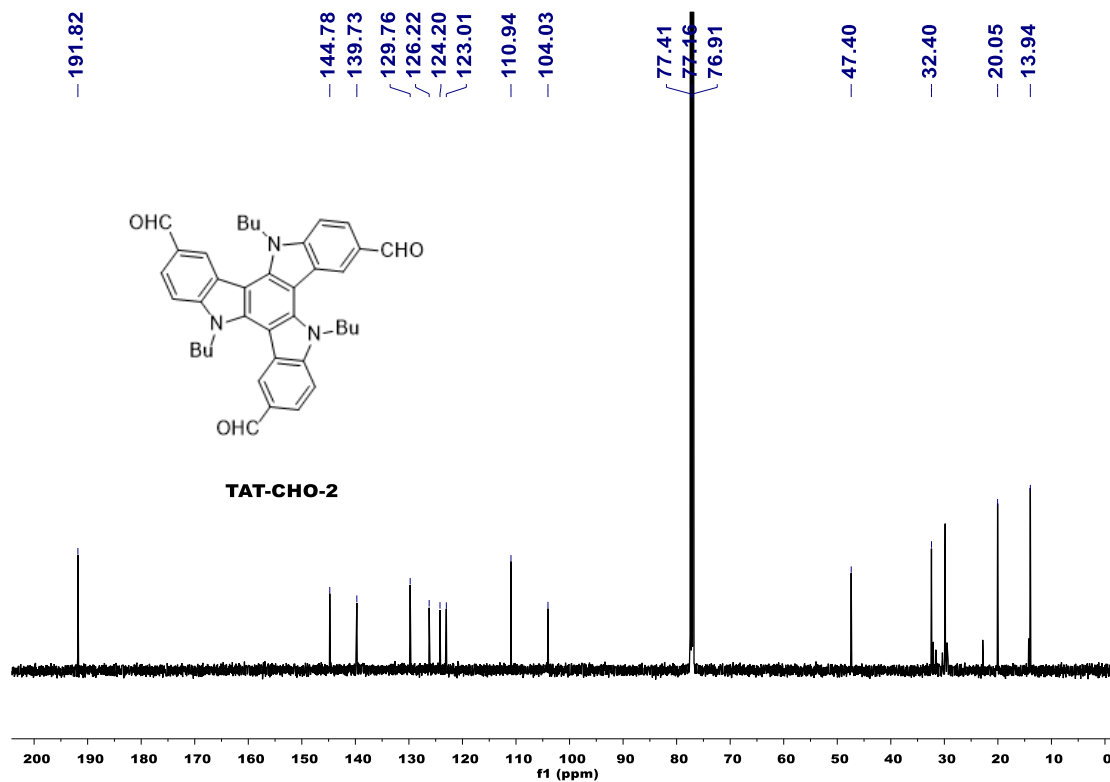


Figure S4. ¹³C NMR spectrum of TAT-CHO-2.

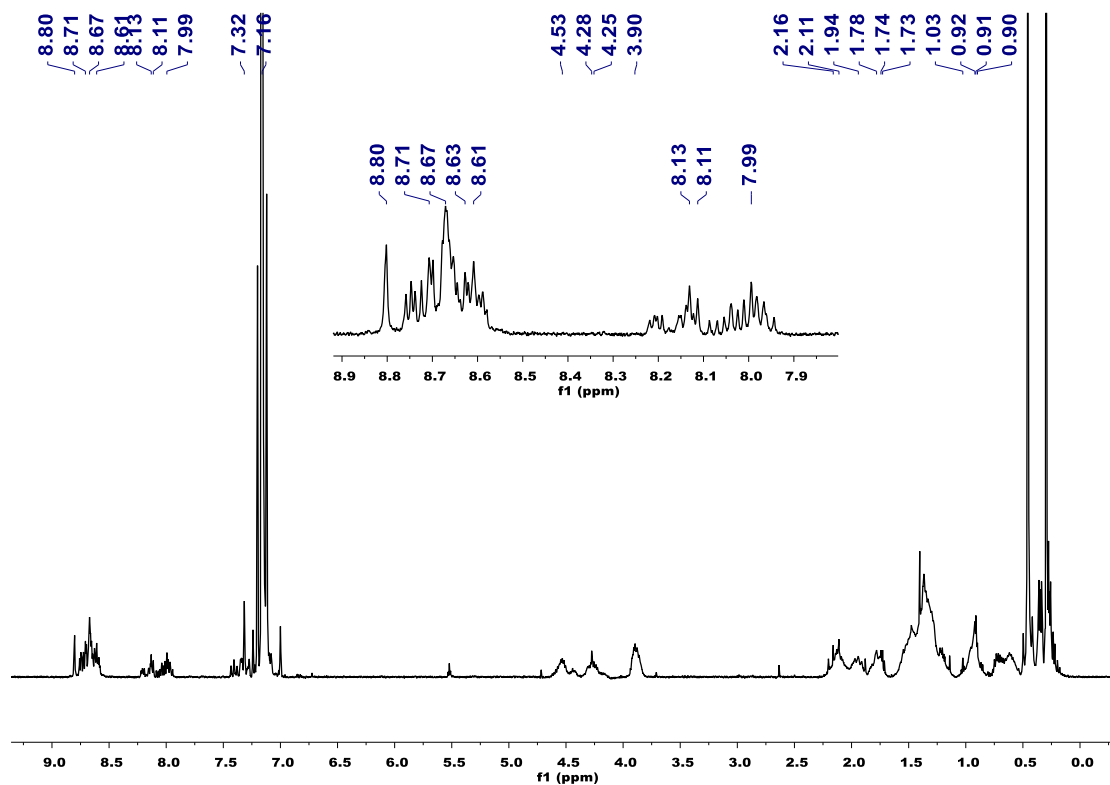


Figure S5. ¹H NMR spectrum of crude FRP-8.

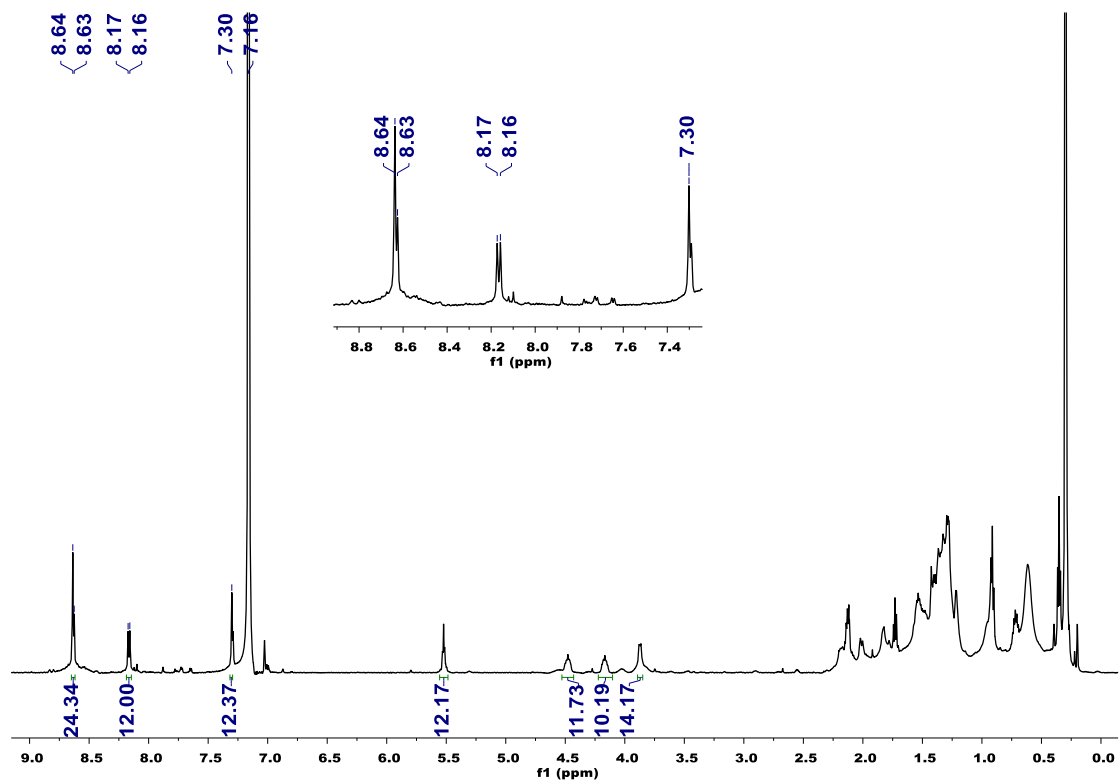


Figure S6. ^1H NMR spectrum of (CCCC)-FRP-8.

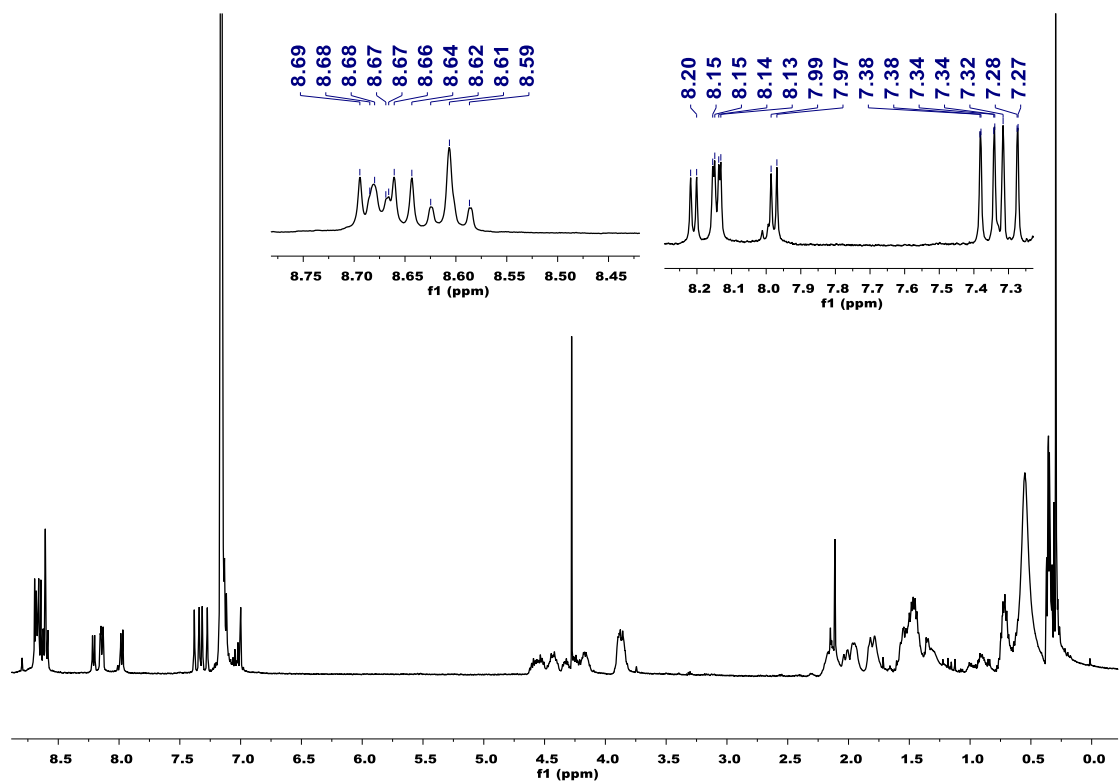


Figure S7. ^1H NMR spectrum of (CCCA)-FRP-8.

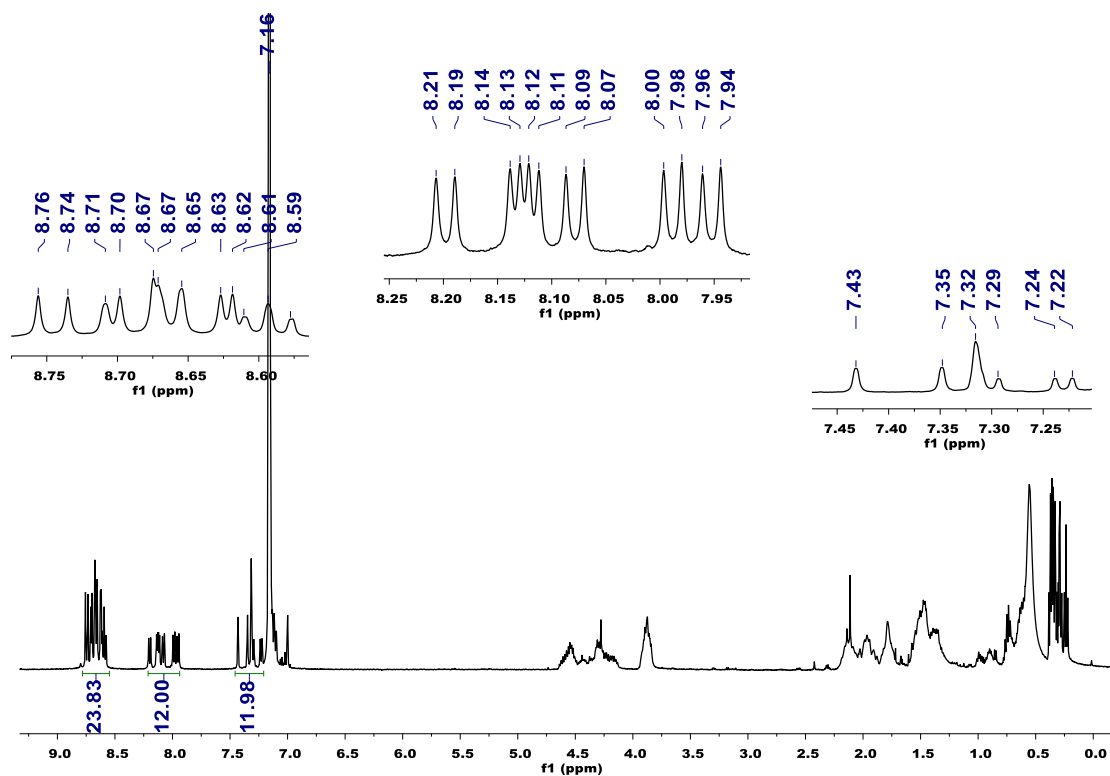


Figure S8. ^1H NMR spectrum of (CAA)-FRP-8.

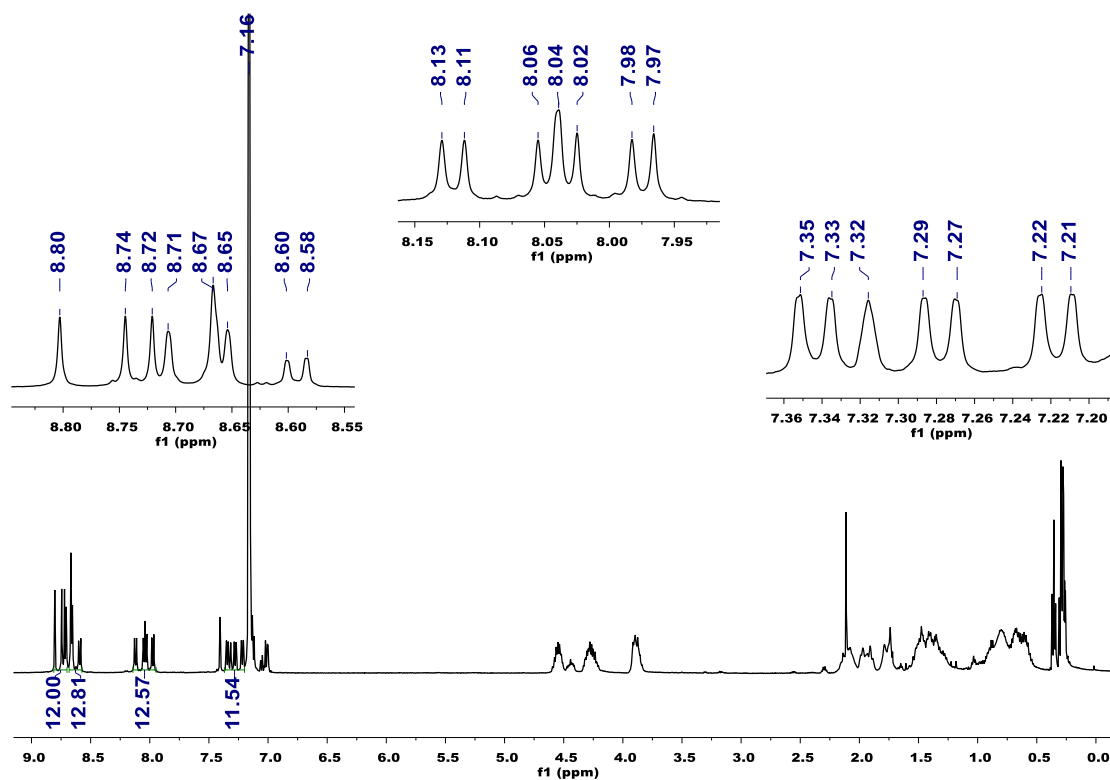


Figure S9. ^1H NMR spectrum of (CAA)-FRP-8.

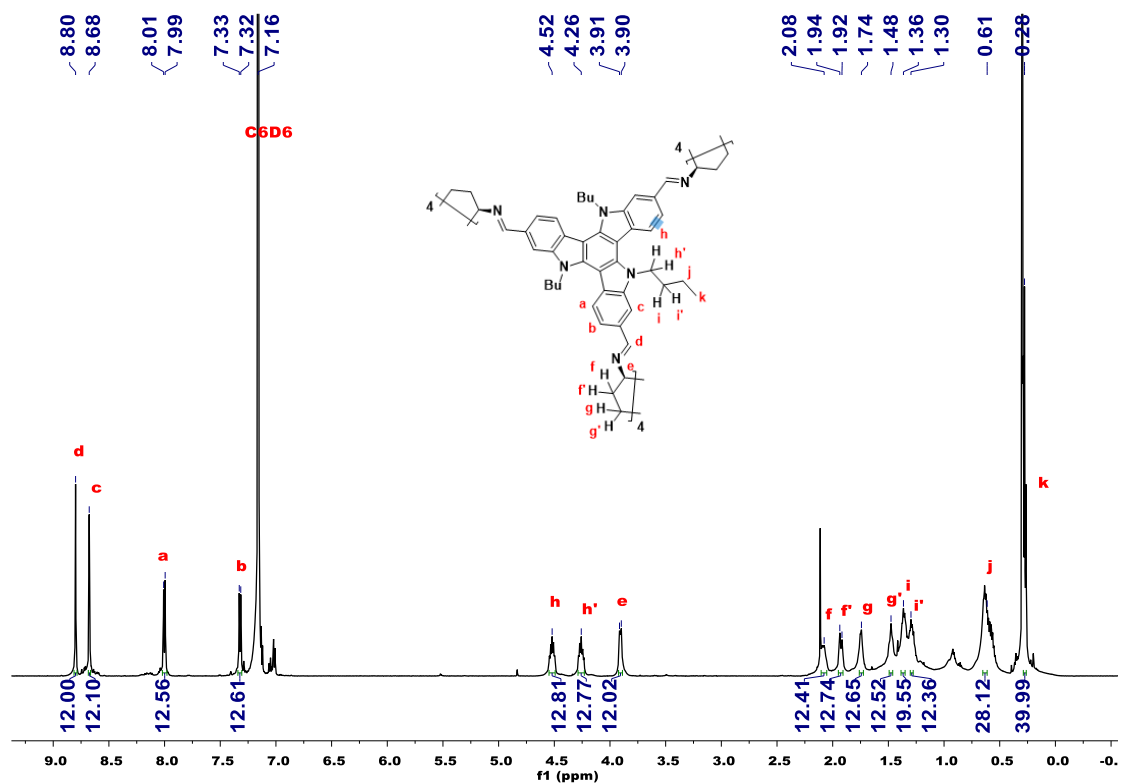


Figure S10. ¹H NMR spectrum of (AAAA)-FRP-8.

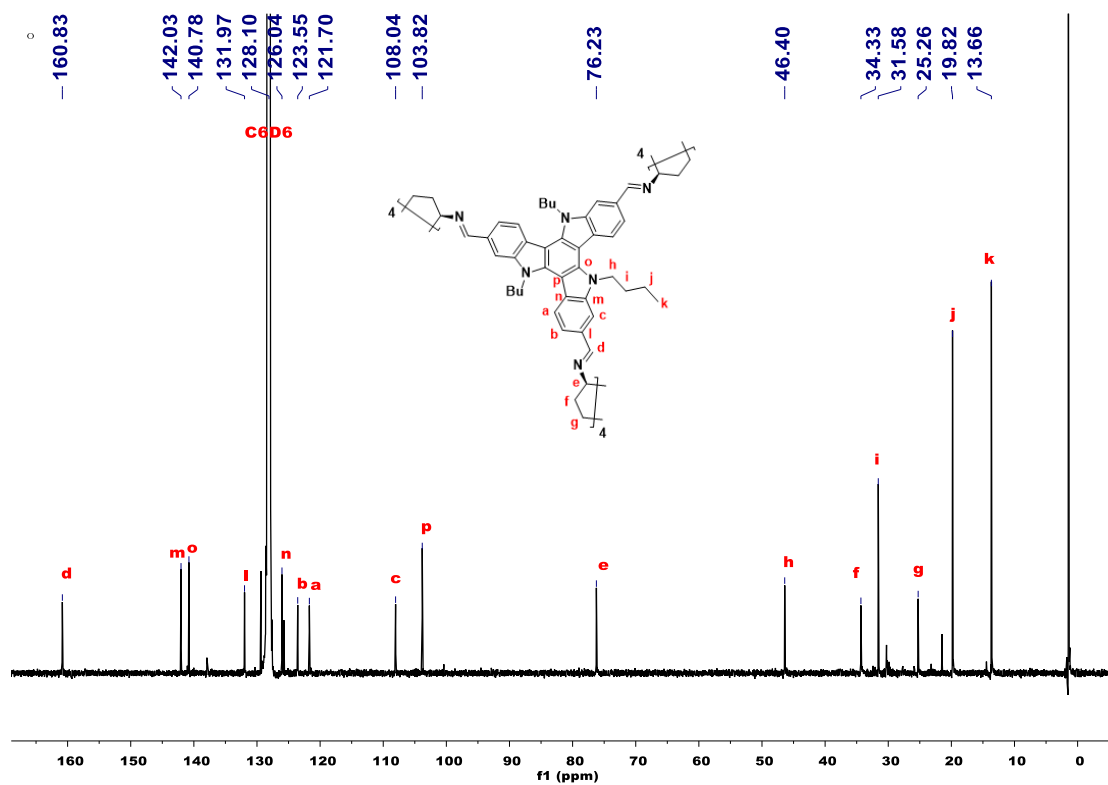


Figure S11. ¹³C NMR spectrum of (AAAA)-FRP-8.

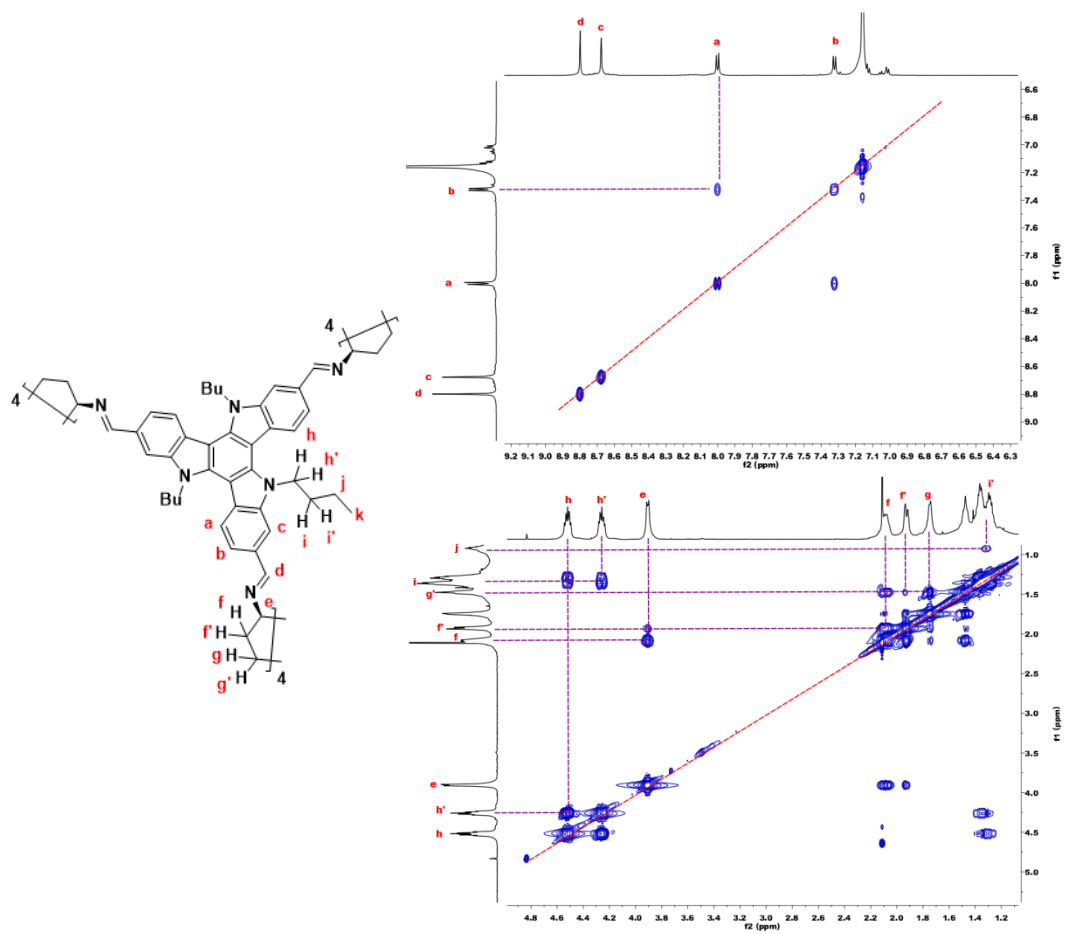


Figure S12. Partial HH COSY spectrum of (AAAA)-FRP-8.

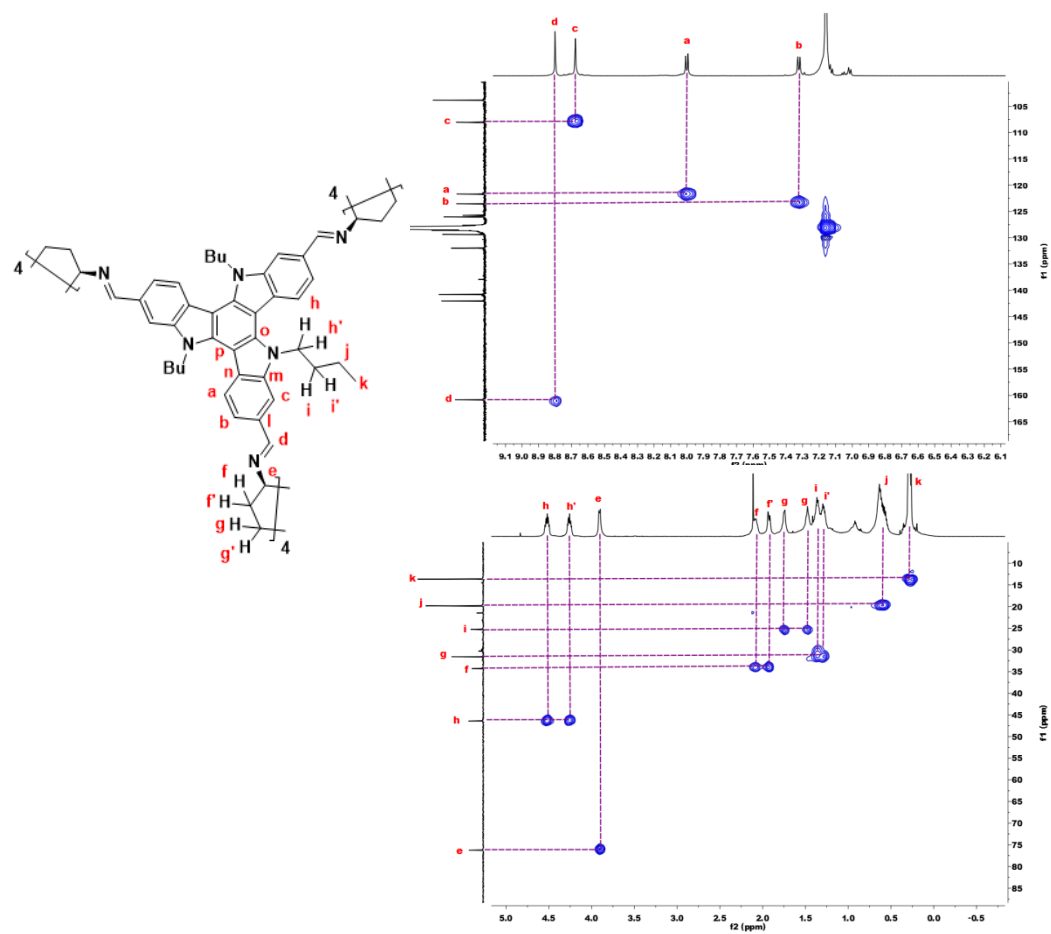


Figure S13. Partial HSQC spectrum of (AAAA)-FRP-8.

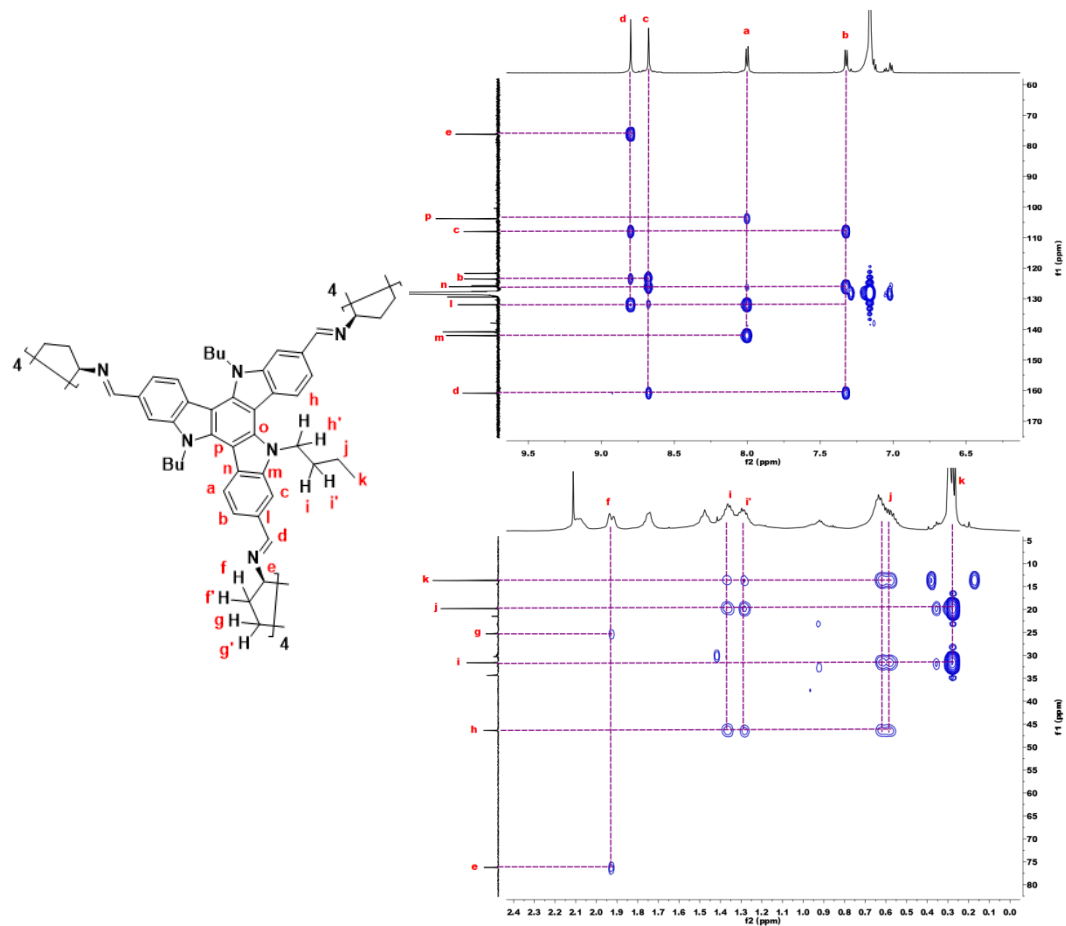


Figure S14. Partial HMBC spectrum of (AAAA)-FRP-8.

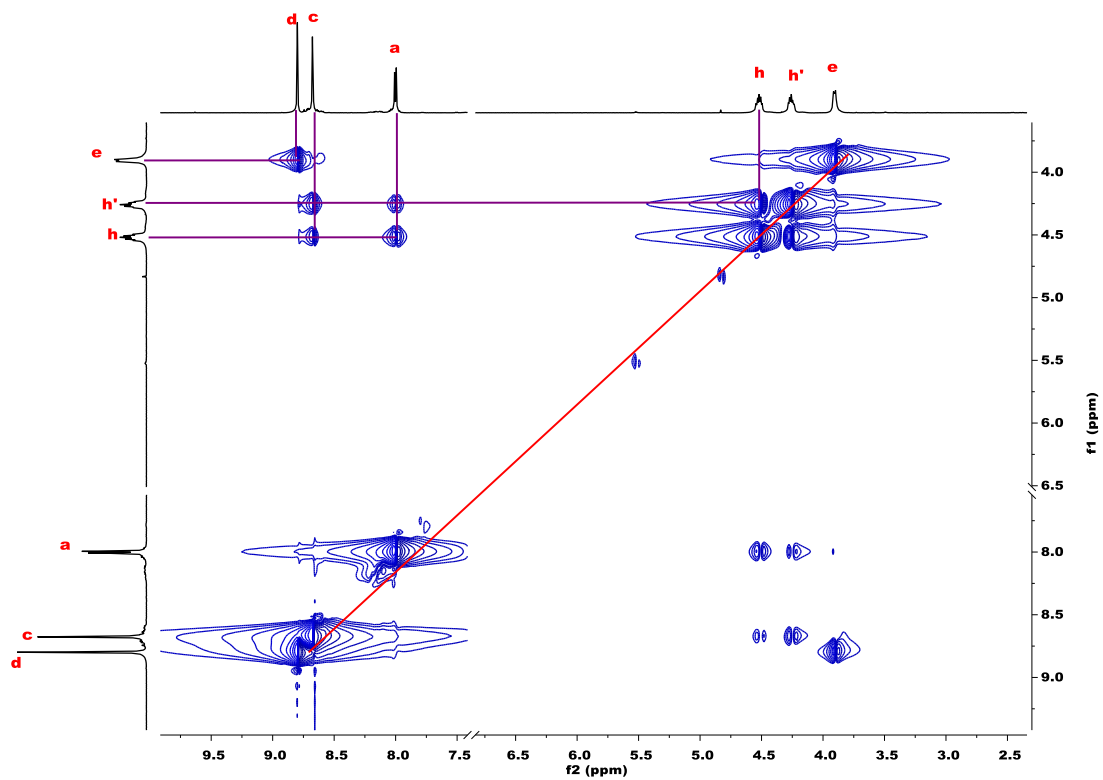


Figure S15. Partial NOESY spectrum of (AAAA)-FRP-8.

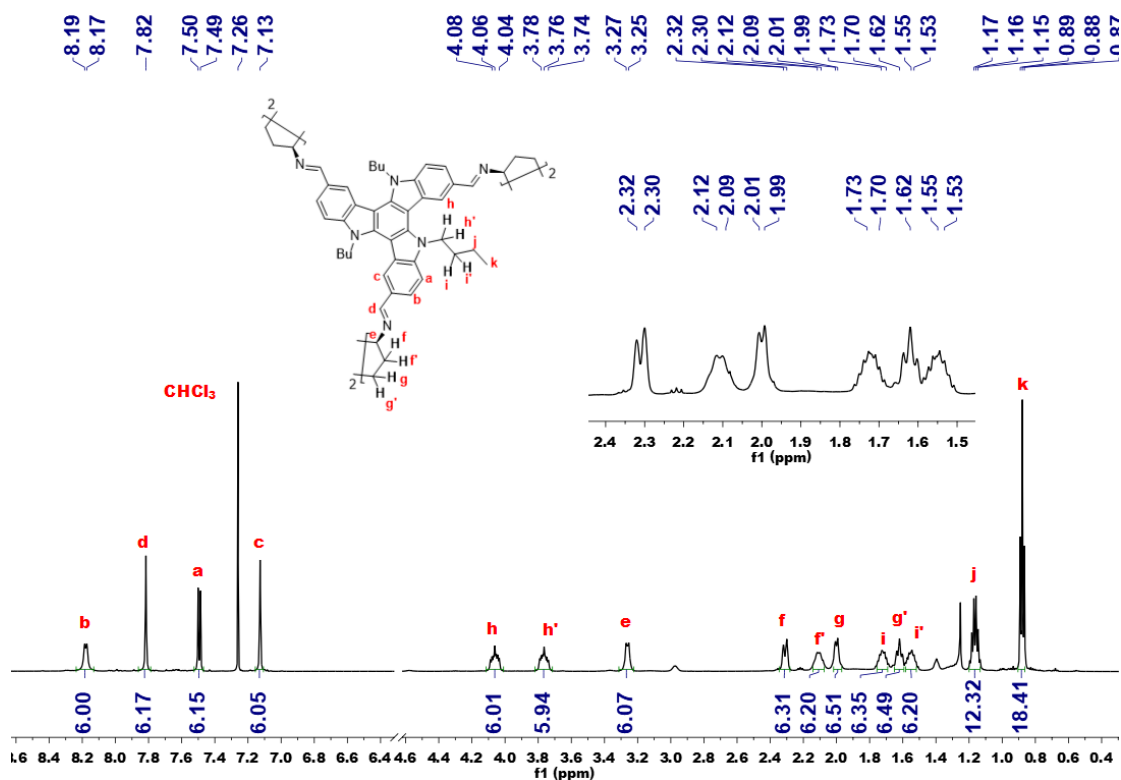


Figure S16. ^1H NMR spectrum of R-FRP-9.

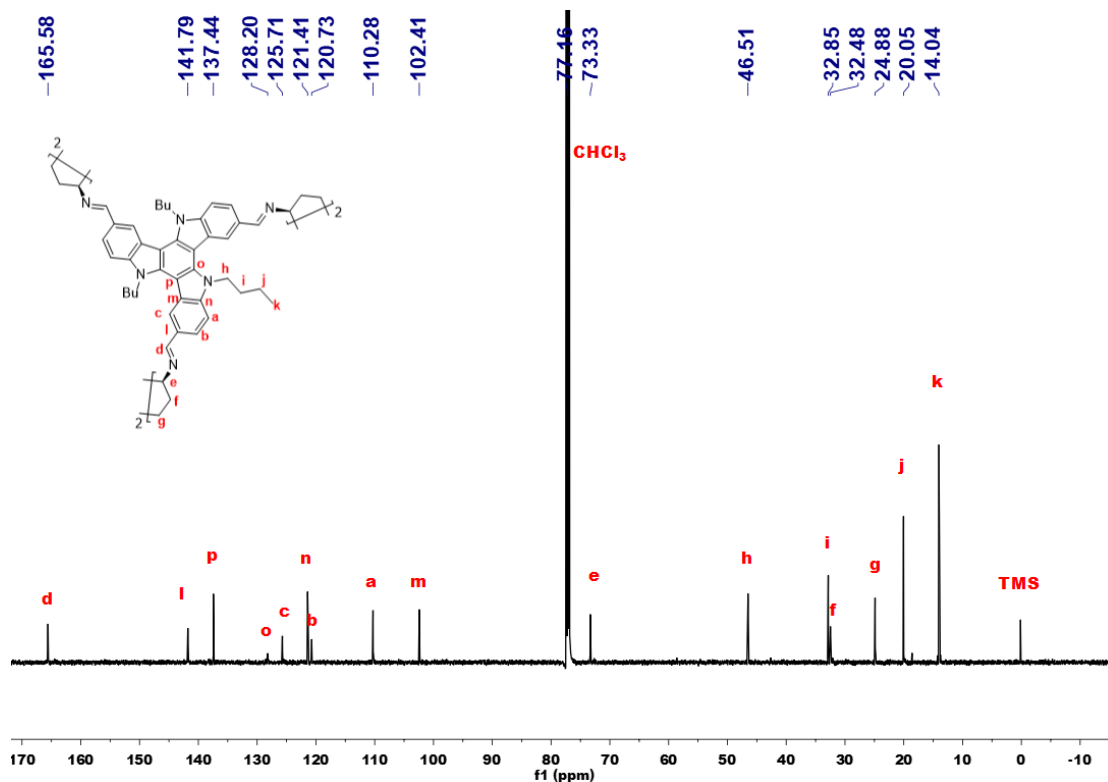


Figure S17. ^{13}C NMR spectrum of R-FRP-9.

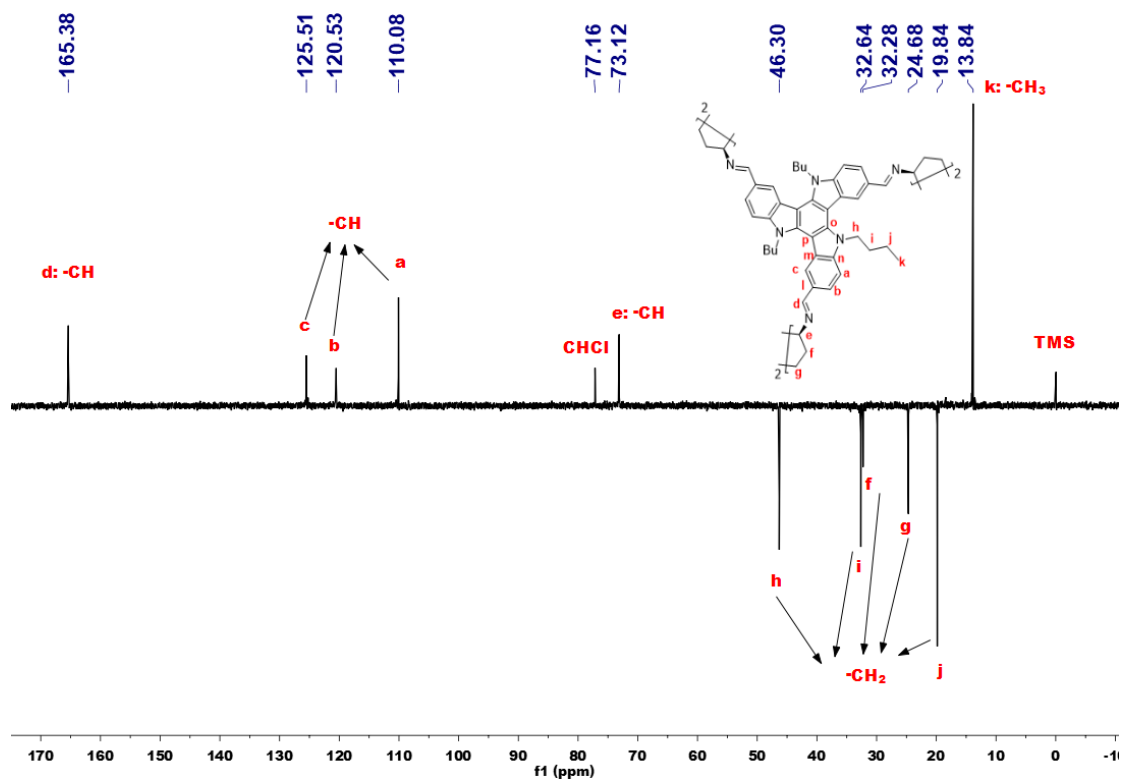


Figure S18. DEPT-135 spectrum of R-FRP-9.

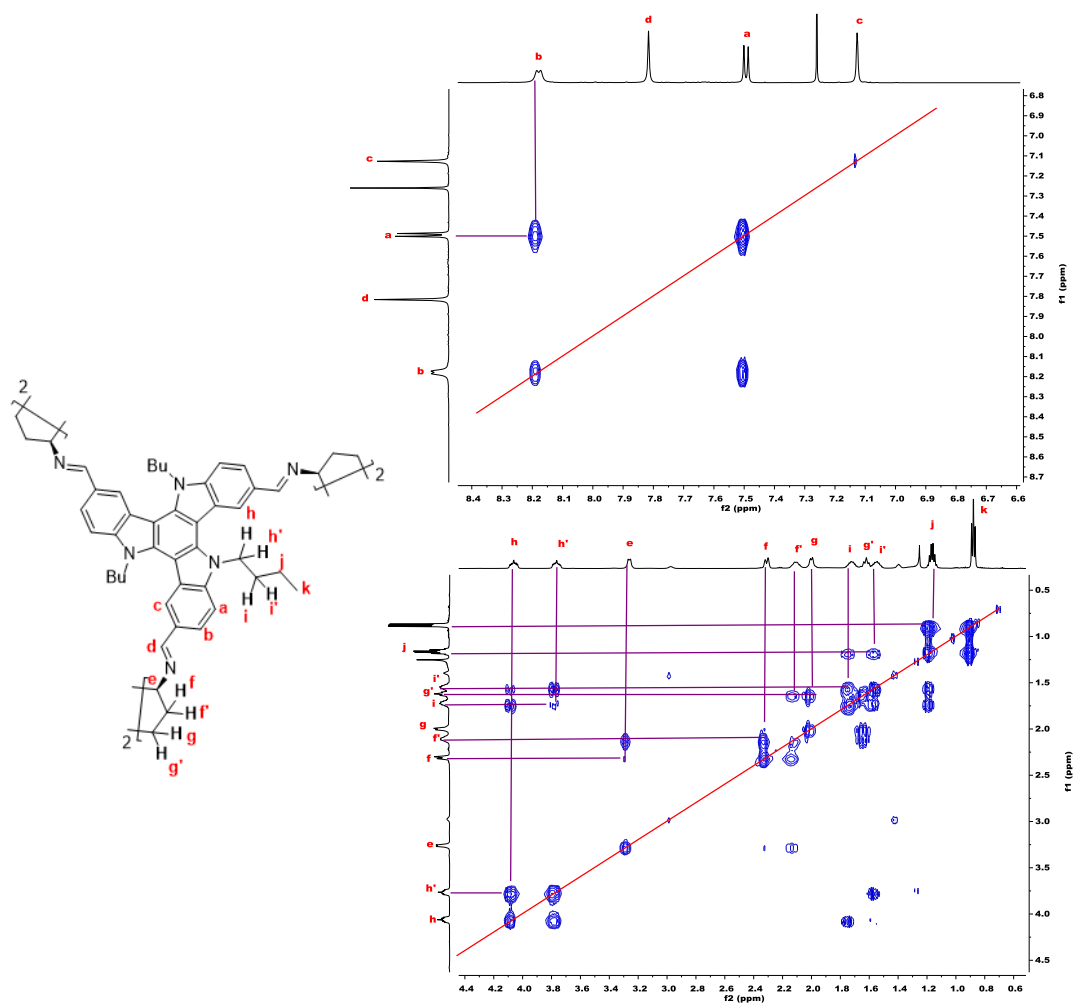


Figure S19. Partial HH COSY spectrum of R-FRP-9.

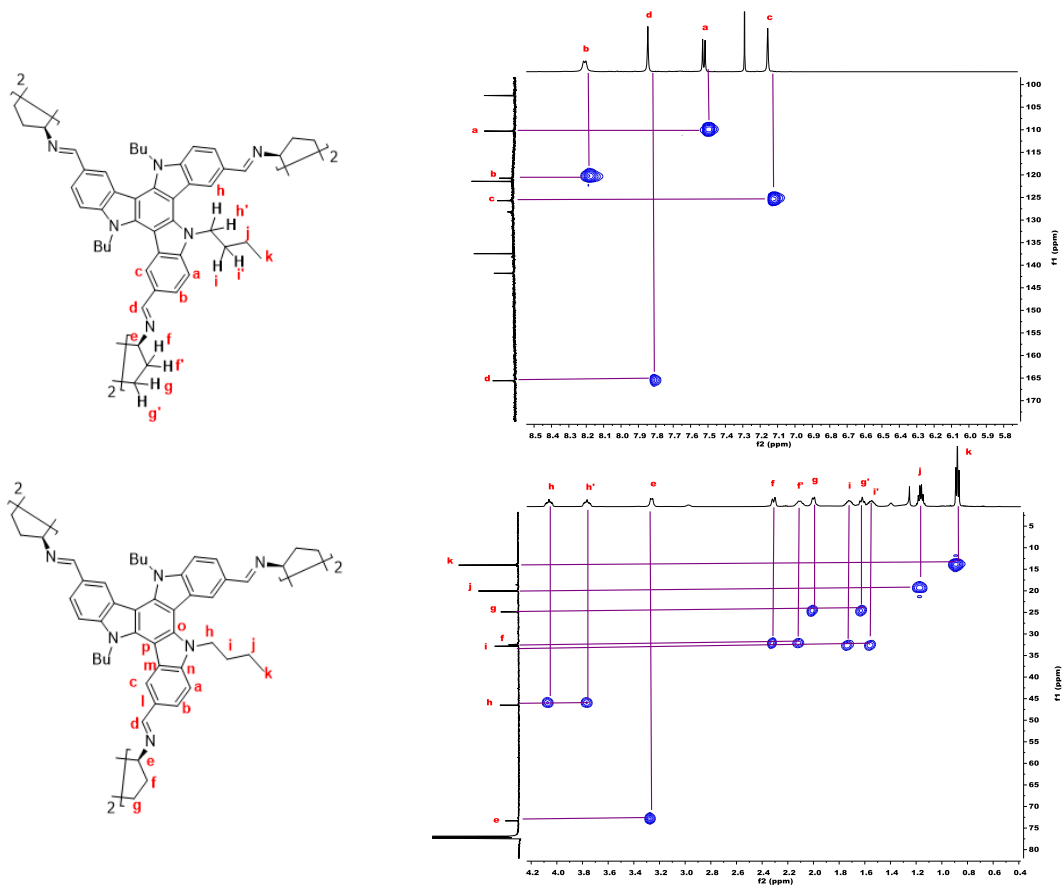


Figure S20. Partial HSQC spectrum of R-FRP-9.

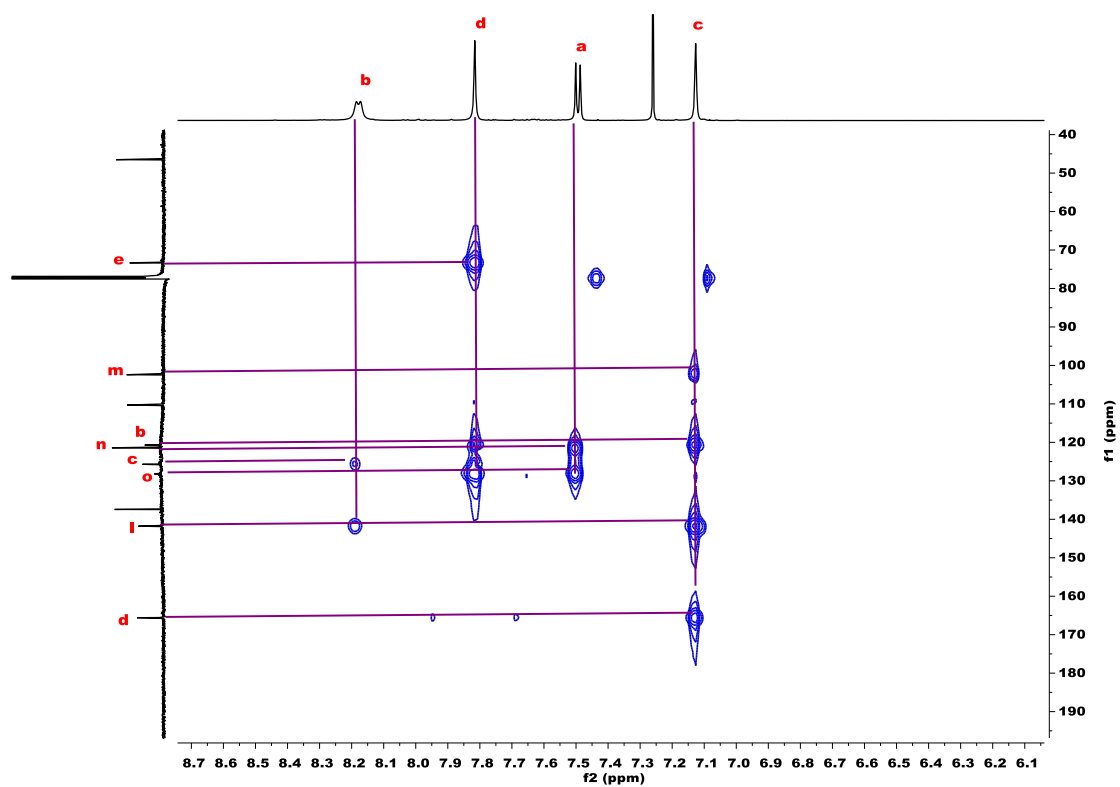


Figure S21. Partial HMBC spectrum of R-FRP-9.

4. HRMS Spectra

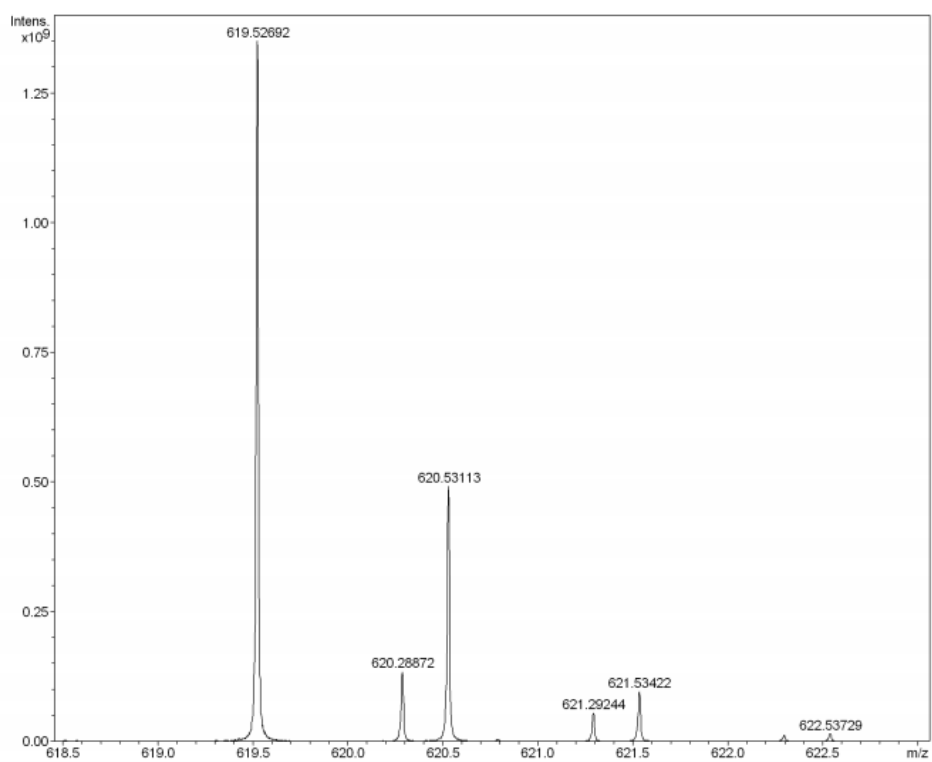


Figure S22. HRMS spectrum of TAT-CHO-1.

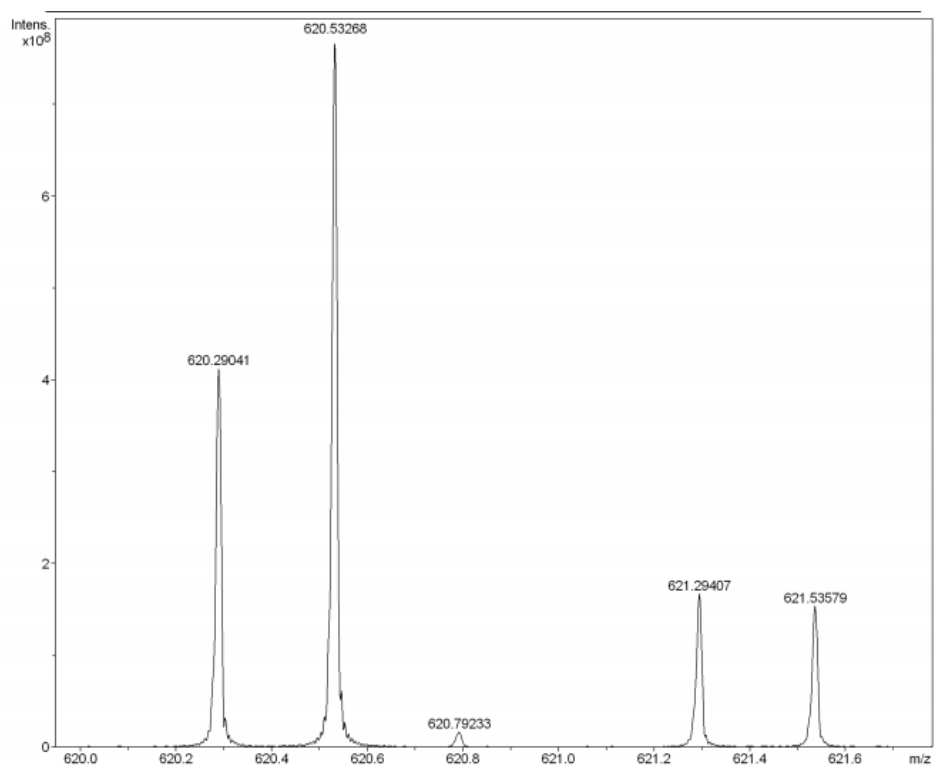


Figure S23. HRMS spectrum of TAT-CHO-2.

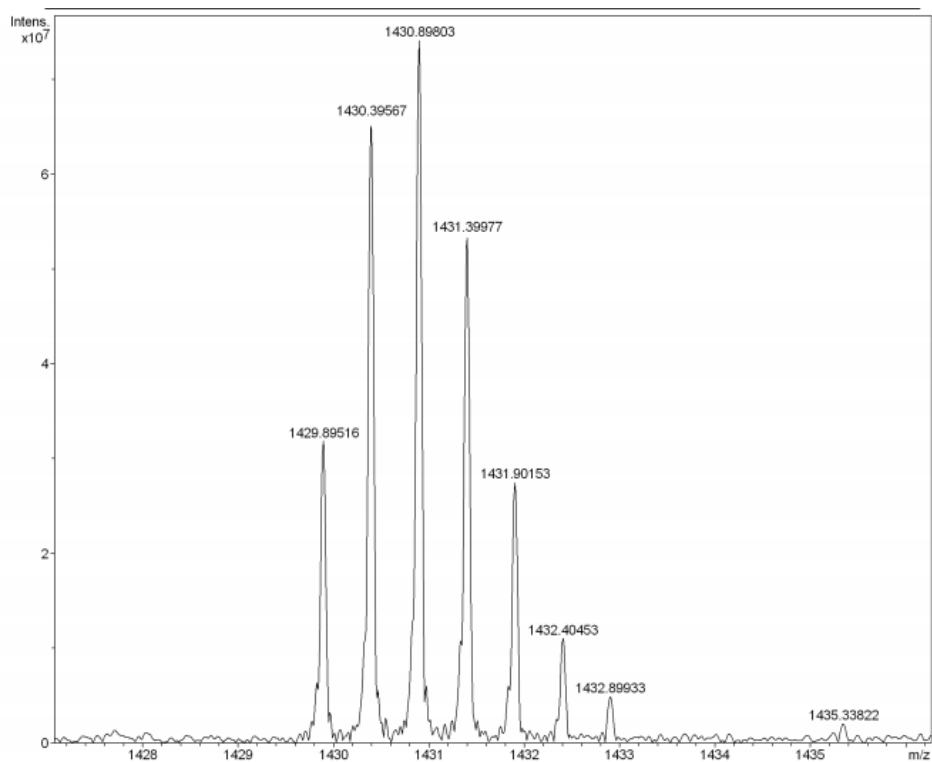


Figure S24. HRMS spectrum of FRP-8.

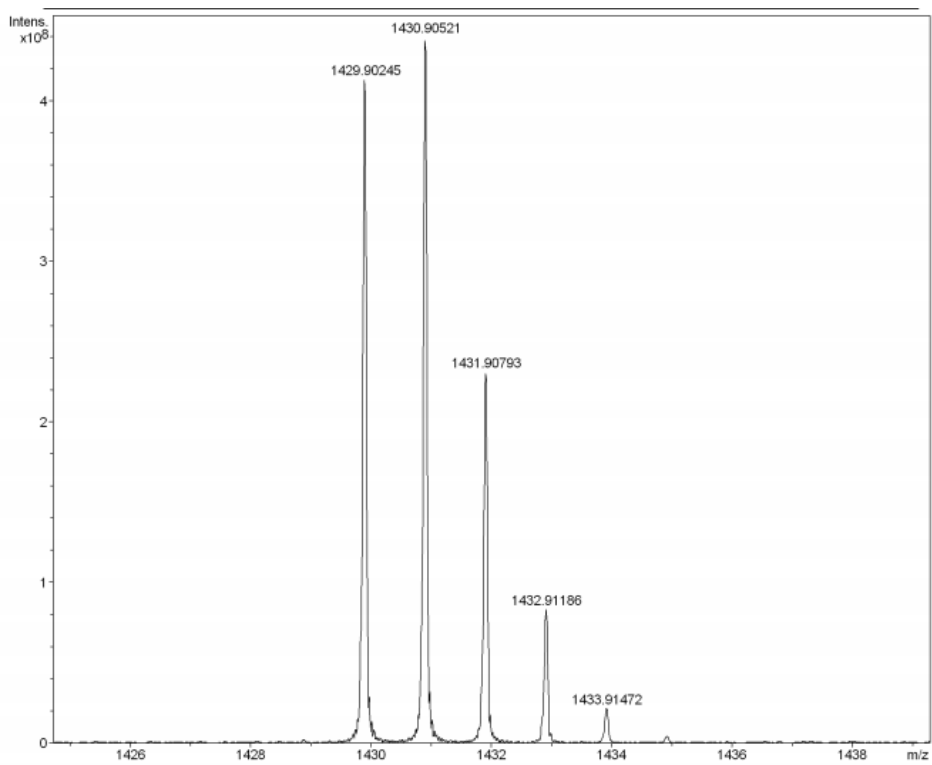


Figure S25. HRMS spectrum of R-FRP-9.

5. HPLC Analysis

HPLC analysis of FRP-9, the eluent is EtOH/hexane=25/75 (v/v). The retention time of R-FRP-9 is 10.377 min, S-FRP-9 is 8.068 min.

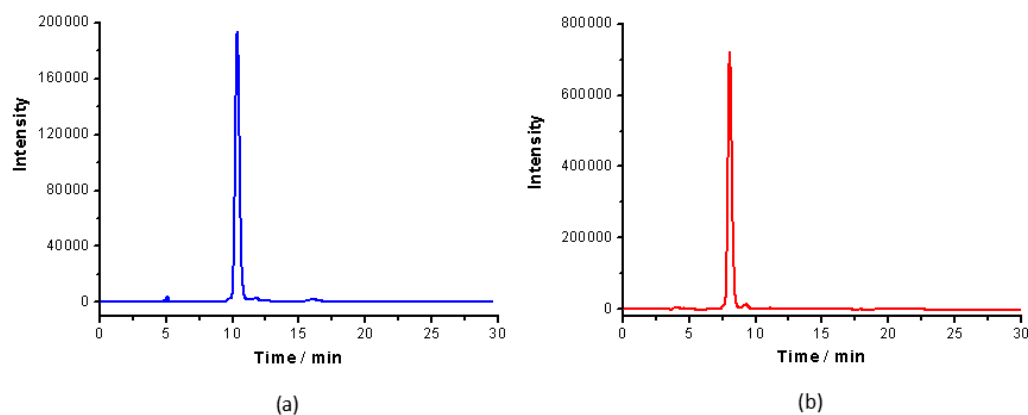


Figure S26. HPLC analysis of FRP-9. (a) R-FRP-9; (b) S-FRP-9.

6. Single Crystal Data

Crystal growing:

The FRP-9 crystals suitable for X-ray analysis were grown by diffusing hexane (3 mL) into high concentration of FRP-9 toluene solutions (10 mg/mL, 1 mL). Transparent hexagonal prisms crystals were grown within two to five days.

Refinement details:

For crystal of R-FRP-9 and S-FRP-9, all non-hydrogen atoms were refined anisotropically. Hydrogen atoms were placed at calculated positions using the riding model and refined isotropically. The instructions AFIX 23 and AFIX 43 were used for the hydrogen atoms on the secondary $-\text{CH}_2-$ and the aromatic C-H, respectively, with the parameter of $U_{\text{iso}}=1.2 U_{\text{eq}}$. The instruction AFIX 33 was used for the hydrogen atoms on the highly disordered terminal $-\text{CH}_3$ groups with the parameter of $U_{\text{iso}}=1.5 U_{\text{eq}}$. No Shelx restraint was applied to the skeleton of the molecular prism, i.e. triazatruxene faces and diamine vertices. Nevertheless, butyl groups are expected to be highly disordered, as they are flexible and would vibrate randomly in the large voids in the crystal. Therefore, necessary Shelx restraints (i.e., DELU, SIMU, and EADP) were applied to the butyl groups to result in a reasonable model. Specifically, the anisotropic displacement parameters of disordered atoms in butyl groups were restrained to be equal within an effective standard deviation of 0.01 using the DELU command. U_{ij} values of disordered atoms of butyl groups were constrained to be similar using the SIMU command. Atomic displacement parameters (ADPs) of different parts of disordered atoms were restrained using the EADP command. There are large voids between the octahedra in crystal, filling with highly disordered solvent molecules. A satisfactory disorder model for the solvent molecules was not found, therefore the OLEX2 Solvent Mask routine (similar to PLATON/SQUEEZE) was used to mask out the disordered density.

Note that, for R-FRP-9 and S-FRP-9, the absolute configuration in crystal was

assigned by reference to an unchanging chiral centre in the assembly procedure, i.e., the chiral carbon atoms of the reagent (1R,2R)-diaminocyclohexane or (1S,2S)-diaminocyclohexane, instead of anomalous dispersion effects in diffraction measurements on the crystal and the derived Flack x parameter. The octahedron crystal contains only light atoms (N, O, C, H) and has large void regions, therefore it is extremely difficult to determine the absolute configuration based on the Flack x parameter with such a large uncertainty. Instead, the diaminocyclohexane reagents used in the assembly procedure have known absolute configurations, and (1R,2R)-diaminocyclohexane or (1S,2S)-diaminocyclohexane does not change its absolute configuration during the assembly process. Therefore, (1R,2R)-diaminocyclohexane or (1S,2S)-diaminocyclohexane fragments can be used as an internal reference to determine the absolute configurations of the molecular prism.

| | |
|--|--|
| Empirical formula | C ₁₄₄ H ₁₆₂ N ₁₈ |
| Formula weight | 2144.91 |
| Temperature/K | 150.00(10) |
| Crystal system | hexagonal |
| Space group | P6 ₁ 22 |
| a/Å | 23.3698(13) |
| b/Å | 23.3698(13) |
| c/Å | 89.848(3) |
| α /° | 90 |
| β /° | 90 |
| γ /° | 120 |
| Volume/Å ³ | 42496(5) |
| Z | 12 |
| ρ_{calc} /cm ³ | 1.006 |
| μ /mm ⁻¹ | 0.456 |
| F(000) | 13824.0 |
| Crystal size/mm ³ | 0.3 × 0.3 × 0.1 |
| Radiation | CuK α (λ = 1.54178) |
| 2 θ range for data collection/° | 5.878 to 136.47 |
| Index ranges | -19 ≤ h ≤ 28, -28 ≤ k ≤ 28, -108 ≤ l ≤ 66 |
| Reflections collected | 98431 |
| Independent reflections | 25951 [R _{int} = 0.0907, R _{sigma} = 0.0742] |
| Data/restraints/parameters | 25951/69/1484 |
| Goodness-of-fit on F ² | 0.942 |
| Final R indexes [I >= 2 σ (I)] | R ₁ = 0.0995, wR ₂ = 0.2700 |
| Final R indexes [all data] | R ₁ = 0.1344, wR ₂ = 0.3208 |

| | |
|---|------------|
| Largest diff. peak/hole / e Å ⁻³ | 0.25/-0.22 |
| Flack parameter | 0.0(4) |
| CCDC number | 1578604 |

Table S1. Single crystal structural determination of R-FRP-9.

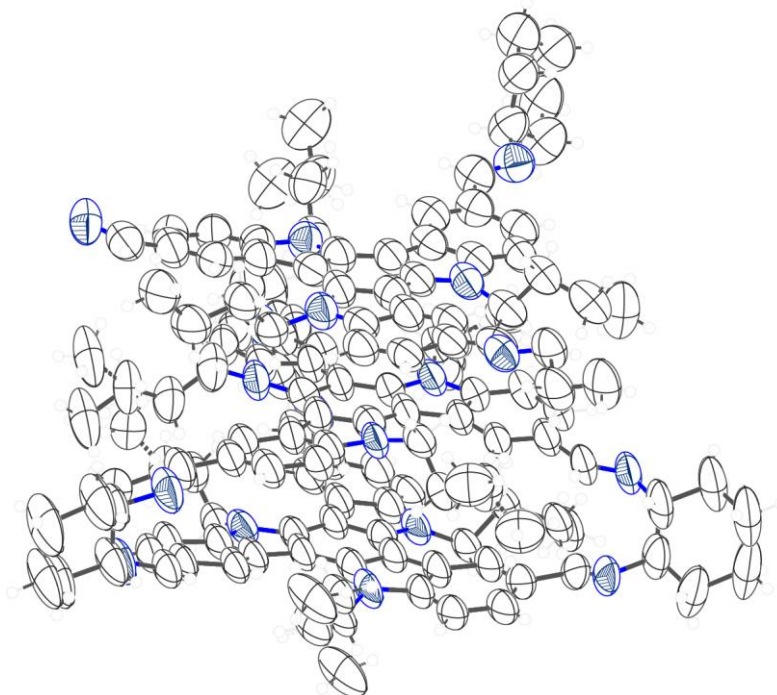


Figure S27. ORTEP drawing of crystal structures of R-FRP-9 (displacement ellipsoids for all non-H atoms at the 50% probability level).

| | |
|---|--|
| Empirical formula | C ₉₆ H ₁₀₈ N ₁₂ |
| Formula weight | 1429.94 |
| Temperature/K | 150 |
| Crystal system | hexagonal |
| Space group | P6 ₅ 22 |
| a/Å | 23.3854(7) |
| b/Å | 23.3854(7) |
| c/Å | 89.444(2) |
| α/° | 90 |
| β/° | 90 |
| γ/° | 120 |
| Volume/Å ³ | 42361(3) |
| Z | 18 |
| ρ _{calc} /cm ³ | 1.009 |
| μ/mm ⁻¹ | 0.458 |
| F(000) | 13824.0 |
| Crystal size/mm ³ | 0.4 × 0.3 × 0.2 |
| Radiation | CuKα (λ = 1.54178) |
| 2θ range for data collection/° | 5.888 to 145.944 |
| Index ranges | -11 ≤ h ≤ 28, -25 ≤ k ≤ 27, -110 ≤ l ≤ 107 |
| Reflections collected | 93184 |
| Independent reflections | 27811 [R _{int} = 0.0819, R _{sigma} = 0.0741] |
| Data/restraints/parameters | 27811/52/1476 |
| Goodness-of-fit on F ² | 1.070 |
| Final R indexes [I ≥ 2σ (I)] | R ₁ = 0.0891, wR ₂ = 0.2366 |
| Final R indexes [all data] | R ₁ = 0.1154, wR ₂ = 0.2613 |
| Largest diff. peak/hole / e Å ⁻³ | 0.39/-0.21 |
| Flack parameter | 0.2(2) |
| CCDC number | 1578652 |

Table S2. Single crystal structural determination of S-FRP-9.

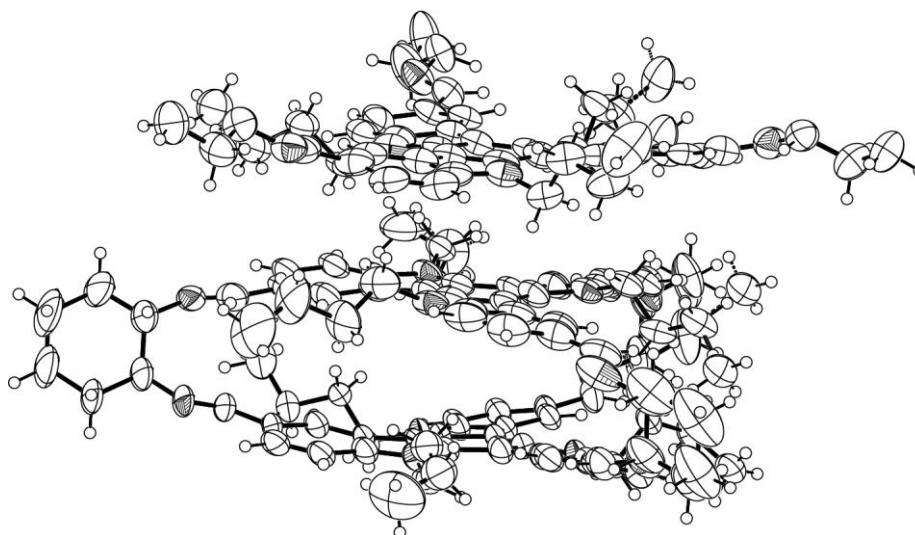


Figure S28. ORTEP drawing of crystal structures of S-FRP-9 (displacement ellipsoids for all non-H atoms at the 50% probability level).

7. Reference

1. Xie, Y.-F.; Ding, S.-Y.; Liu, J.-M.; Wang, W.; Zheng, Q.-Y., Triazatruxene based covalent organic framework and its quick-response fluorescence-on nature towards electron rich arenes. *J. Mater. Chem. C* **2015**, *3* (39), 10066-10069.
2. Ji, L.; Fang, Q.; Yuan, M.-S.; Liu, Z.-Q.; Shen, Y.-X.; Chen, H.-F., Switching High Two-Photon Efficiency: From 3,8,13-Substituted Triindole Derivatives to Their 2,7,12-Isomers. *Org. Lett.* **2010**, *12* (22), 5192-5195.
3. Krick, M.; Holstein, J.; Wuertele, C.; Clever, G. H., Endohedral dynamics of push-pull rotor-functionalized cages. *Chem. Commun. (Cambridge, U. K.)* **2016**, *52* (68), 10411-10414.
4. Shao, J.; Guan, Z.; Yan, Y.; Jiao, C.; Xu, Q.-H.; Chi, C., Synthesis and Characterizations of Star-Shaped Octupolar Triazatruxenes-Based Two-Photon Absorption Chromophores. *The Journal of Organic Chemistry* **2011**, *76* (3), 780-790.
5. Wang, X.; Wang, Y.; Yang, H.; Fang, H.; Chen, R.; Sun, Y.; Zheng, N.; Tan, K.; Lu, X.; Tian, Z.; Cao, X., Assembled molecular face-rotating polyhedra to transfer chirality from two to three dimensions. *Nat. Commun.* **2016**, *7*, 12469pp.